HRL Technology Pty Ltd
ABN 95 062 076 199

The energy experts

Part of the HRL group of companies

Level 1, Unit 9
677 Springvale Road
Mulgrave 3170
VIC Australia

Ph: +61 3 9565 9888
Fax: +61 3 9565 9866
Email: info@hrl.com.au
www.hrlt.com.au

Prepared for

Brown Coal Innovation Australia

Advanced Materials Assessment Program Summary Report

Report No: HLC/2012/128

April 2012

CONFIDENTIAL - CLIENT USE ONLY

by

Dick Coldham

Initial Distribution

Advanced Materials Assessment Program Project Partners

Phil Gurney	BCIA
David McManus	BCIA
Stuart Mann	Loy Yang Power
Steve Pascoe	TRUenergy
Mark Rooney	IP GDF SUEZ Loy Yang B
Kim Hayes	IP GDF SUEZ Loy Yang B
Garry Smith	IP GDF SUEZ Loy Yang B
Tanveer Hasan	IP GDF SUEZ Hazelwood
Raman Singh	Monash University

HRL Technology Pty Ltd

HRL Report Archive
File: 82100023

Revision	Date	Reviewed by	Approved by	Comment
-	23/04/2012	D. O'Neill, A. Czerwinski	H. Sinclair	

Table of Contents

1 Introduction

Victorian base-load brown coal-fired power stations are ageing, with the oldest larger conventional units now approaching 40 years of service. The newest station was commissioned 16 years ago. The station components operate at elevated temperatures and high pressures and deteriorate with age. This increases the risk of failure and the requirements for significant maintenance or upgrade of components. The conventional materials used in Latrobe Valley power stations limit the final steam temperature to around 540°C, and hence restrict maximum plant efficiency. Over the past twenty years there have been major developments in the alloys available for power generation, following the demand for increased steam temperatures. Super critical units currently in service operate at 600°C and above and major international programs are targeting final steam temperatures of 700°C for ultra-super critical units. The Victorian government recognised the need for improvements in the knowledge base associated with the high temperature alloys used in power generation. To this end under the Department of Primary Industry Energy Technology Innovation Strategy (ETIS) funding was provided for the Advanced Materials Assessment Program. The original ETIS program ran for approximately three years, but because of the long-term nature of much of the testing there was perceived value in continuing the program. Additional funding for research into the high temperature deterioration of alloy steels was provided through Brown Coal Innovation Australia (BCIA), for a further 18 months research.

The underlying objective of the ETIS/BCIA research program was to improve knowledge of the advanced materials for power plant and to improve techniques for their assessment and repair. The work was seen to facilitate the introduction of improved materials without increasing risks to plant or personnel. The project was undertaken in four strands, each addressing different aspects in the evaluation of materials:

Strand 1	Understanding oxide growth kinetics in a steam environment and developing improved algorithms relating oxide thickness to operating temperature for alloy steels, including 9% and 12% chromium steels
Strand 2	Characterisation of microstructure changes of ferritic and austenitic steels as a function of ageing, to assess the fitness for service of materials and components.
Strand 3	Developing improved creep testing techniques to provide more rapid and accurate prediction of life of plant, with particular focus on the measurement of creep strain rate as an indicator of remaining life.
Strand 4	Evaluating improved welding techniques to reduce outage times, specifically by comparing the creep properties of flux-core versus conventional weld repairs and evaluating the risks of using the more rapid flux core techniques.

Full reports[1] have been prepared on each of the program strands. This report provides an extended summary of the research that has been carried out under the ETIS and BCIA programs and presents some of the pertinent results from each Strand.

[1] Oxide Growth Kinetics – Andrew Czerwinski HRL Report No. HLC/2012/129
Microstructural Changes in High Temperature Alloy Steels – Sky Loo and Russell Coade HLC/2012/130
Creep Strain Assessment – Marc Listmangof HRL Report No HLC/2012/131
Advanced Weld Repair – Russell Coade & Dick Coldham HRL Report No. HLC/2012/132

2 Objectives of the program

The aims of the ETIS-BCIA Advanced Materials Assessment Program were to:-

- Improve our knowledge of conventional and advanced materials for power plant applications
- Accelerate the introduction of new materials without increasing risk to the plant or personnel.
- Contribute to greenhouse gas reduction through an understanding of the new generation materials that may encourage and accelerate their introduction to Victorian and Australia plant. This would enable operating temperatures and pressures to increase, and lead to an increase in plant efficiencies.
- Improve plant life, safety and asset utilisation through improvements in life assessment methods.
- Increase the knowledge and experience of young engineers working in the power generation and related businesses.

3 Project achievements

(i) Development of knowledge concerning the performance and assessment of high temperature alloys used in power stations and increasing skill levels in young engineers. Three graduate engineers were involved for a large percentage of their time and one is in the process of transferring from a Master of Engineering Science program to PhD for aspects of work on oxidation.

(ii) Commissioning of a unique, world class steam oxidation testing facility simulating power plant conditions (at Loy Yang B power station) and the establishment of a laboratory scale steam oxidation test facility at Monash University.

(iii) Proficiency using upgraded equipment for non-destructively measuring the thickness of oxides on the bore of steam tubing with sophisticated software for metal temperature estimation and life assessment.

(iv) Availability of thermally aged and creep damaged CMV and 2¼Cr1Mo ex-service material that has been fully characterised for further testing programs and the validation of new techniques.

(v) Availability of creep damaged materials with welds from different procedures, from which additional test samples can be extracted and used to fully evaluate potential problems of welding repairs.

(vi) Commissioning of advanced creep testing equipment with capability to conduct measurement of creep strain rate for improved life assessment. The facility can also be used for creep-fatigue testing, to explore the effects of cyclic operation, and stress relaxation testing used specifically in assessment of the safe operating life of turbine bolting.

(vii) Installation of an additional suite of miniature creep rupture test machines, with argon shielding gas to minimise sample oxidation. This significantly expands capacity for long term tests.

(viii) Development and validation of models for oxide growth on high chromium and advanced ferritic steels used in power plant environments.

(ix) Atlas of microstructure transitions during the ageing of ferritic and austenitic steels over a range of temperatures.

(x) An atlas of oxide morphology for scales grown in steam at temperatures from 600°C to 800°C.

(xi) Increased knowledge of the behaviour of new high temperature alloys, potential problems with these materials and how to evaluate their condition.

4 Benefits to participants

(i) New oxide thickness equipment and improved protocol for converting oxide thickness into metal temperature.

(ii) Oxide thickness surveys at Yallourn and Loy Yang A to determine metal temperature distributions across superheater and reheater tubing.

(iii) A technique to accelerate testing to determine the remaining creep life of high temperature components, with assessments available from ~1,000 hours of testing rather than over a year.

(iv) Improved assessment techniques to determine fitness for service of aged material from NDT including replicated microstructure and in situ hardness testing.

(v) Data on the creep performance of flux-cored weld repairs suggests that this procedure could be used as an alternative to conventional manual metal arc welding in some instances though longer term creep evaluation is required.

(vi) More detailed understanding of the life of temper bead weld repairs in 2¼Cr1Mo and CMV materials compared with conventional heat treatment in weld repairs.

(vii) More information on the risks of weld cracking in CMV materials (which are widely used in the Latrobe Valley) as components exceed 200,000 hours service and of appropriate techniques to manage risk.

(viii) Availability of thick walled weld samples for additional testing and assessment activities.

(ix) Technical committee meeting that have provided a forum for discussing problems and sharing technical information between Latrobe Valley power generators.

5 Additional research and testing

The research undertaken under the Advanced Materials Assessment Program has been extensive and has generally achieved the goals. There are some areas, however, where further investigations would improve confidence in the results to date, and allow some of the potential technologies to be introduced with minimal and known risk. Opportunities include:

Oxidation kinetics – This work has been used as part of a post-graduate Masters of Engineering Science project at Monash University, and under that project more detailed evaluation of data and improvements in the understanding and modelling of oxidation kinetics will be carried out. The work completed to date has been assessed by the University and they have expressed the opinion that with some slight expansion of scope this work would be suitable for transfer to a PhD thesis. This is currently under consideration.

Creep-strain Additional creep-strain testing would greatly improve confidence in the applicability of the two methods of data evaluation to determine remaining life of plant and materials operating at high temperatures. As these methods have the potential to provide accurate estimates of life based on only one (or perhaps duplicate) short term (~1,000 hour) creep test(s) this would offer considerable benefits to the power generators.

Weld repair Relatively short term creep-rupture testing confirmed that the creep strength of repair welds using the flux cored procedure, with high rates of metal deposition and short weld times, were consistent with the properties of conventional manual metal arc welding, and that heat treatment or temper bead procedures produced similar weld strength. Longer term creep-rupture testing for 8,000 to 16,000 hours and preferably longer, is necessary to validate results to date and identify any risks associated with the uptake of this time-saving procedure.

6 Alloy steels used in the program

A schematic showing the development of high temperature alloys for use in power generation over the past 100 years is presented in Figure 1, with the provenance of pertinent steels highlighted. The compositions of alloys selected for the program are shown in Table 1.

Steels T9 and 347H were chosen as they are presently in use in the Latrobe Valley power stations but there is limited data on their oxidation and microstructural response to service. Additionaly steel T9 is the precursor to the more advanced alloys T91 and T92. Steels T23, T91, and 347HFG are next generation steels (2nd generation) that are presently in use in more modern and some super-critical plant in Australia and are expected to be used in new Victorian plant in the coming years. Alloys T92, HR3C, Super304H and AFA are 3rd generation steels that are being developed to be incorporated in future supercritical plant. Not shown in Table 1 is one of the materials used in the welding repair activity. This work included a sample taken from a main steam line manufactured from 0.5Cr 0.5Mo 0.25V (CMV), a cast bifurcation, and similar alloys are in common use for high temperature piping and valves.

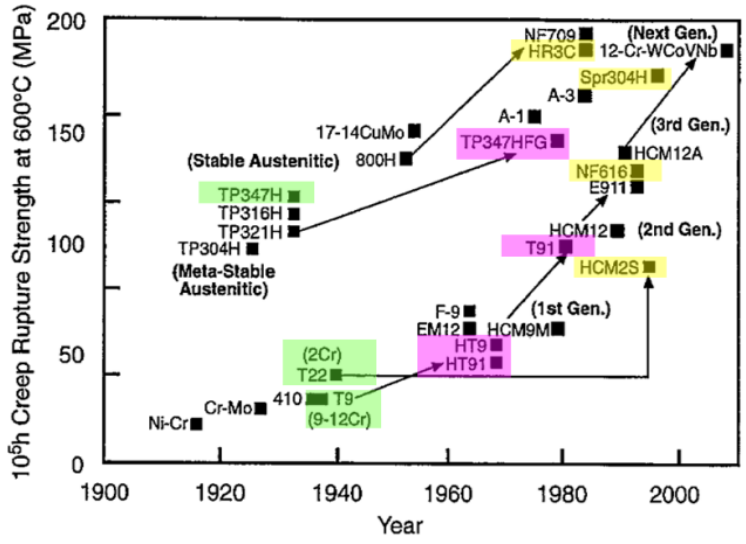

Figure 1 Development of boiler steels. Note that T23 = HCM2S and T92 = NF616

Material	Composition (wt%)											
	C	N	Cr	Ni	Mo	V	Nb	W	Mn	Si	Al	Cu
T23	0.06	-	1.85	0.09	0.14	0.21	0.02	1.93	0.47	0.27	0.03	-
T9	0.10	-	8.45	0.24	0.90	0.03	0.01	-	0.39	0.35	0.02	-
T91	0.07	-	7.66	0.05	0.87	0.20	0.07	0.03	0.42	0.27	0.01	-
T92	0.08	-	8.03	0.23	0.38	0.18	0.04	1.97	0.37	0.48	0.03	-
347H	0.06	-	17.9	10.7	0.20	0.03	0.50	-	1.90	0.22	0.01	-
347HFG	0.08	-	18.4	11.3	<0.01	0.02	0.66	-	1.17	0.32	0.01	-
AFA	0.04	-	14.0	25.0	1.6	-	2.5	-	1.9	0.13-0.15	3.5	-
HR3C	0.09	0.23	24.62	19.42	-	-	0.41	-	1.46	0.62	-	-
SUPER304H	0.10	0.10	18.0	9.0	-	-	0.40	-	0.80	0.20	-	3.0

Table 1: Chemical composition of alloys used in the Advanced Materials Assessment Program

7 Strand 1 - Oxide growth kinetics

The thickness and characteristics of the oxides that develop in-service on boiler and superheater tubing can provide information on the thermal history and operating temperature, and hence provide an essential input to assessment of remaining life of the tube materials and other components. In addition, the formation of excessively thick steam-side oxide is a major problem in power stations worldwide, leading to boiler tube failures by

- short term overheating because the low thermal conductivity of oxide scales impedes heat transfer across tube walls
- loss in metal wall thickness resulting from oxidation that increases hoop stresses and potentially results in creep rupture
- exfoliation of oxide scale resulting in tube blockages, flow restrictions and erosion of downstream plant by hard oxide particles.

Thus, in addition to being able to predict remaining creep life, a detailed knowledge of oxidation kinetics can help determine when exfoliation is likely in order to make provisions for chemical cleaning before it poses a risk to plant.

The primary focus of this aspect of the R&D program involved exposing a number of tube materials to steam at above-design temperatures for periods of up to 12,000 h in order to investigate the rate and type of oxide growth. Testing was carried out concurrently in a simulated steam environment at Monash University, Clayton campus, using an argon/steam mixture, and using live steam from the hot reheat line at Loy Yang B (LYB) power station in the Latrobe Valley. A schematic of the LYB setup is shown in Figure 2a and the facility can be seen in Figure 2b. The installation operated at the reheat pressure of 4.2 MPa and therefore necessarily complied with a full suite of OH&S requirements.

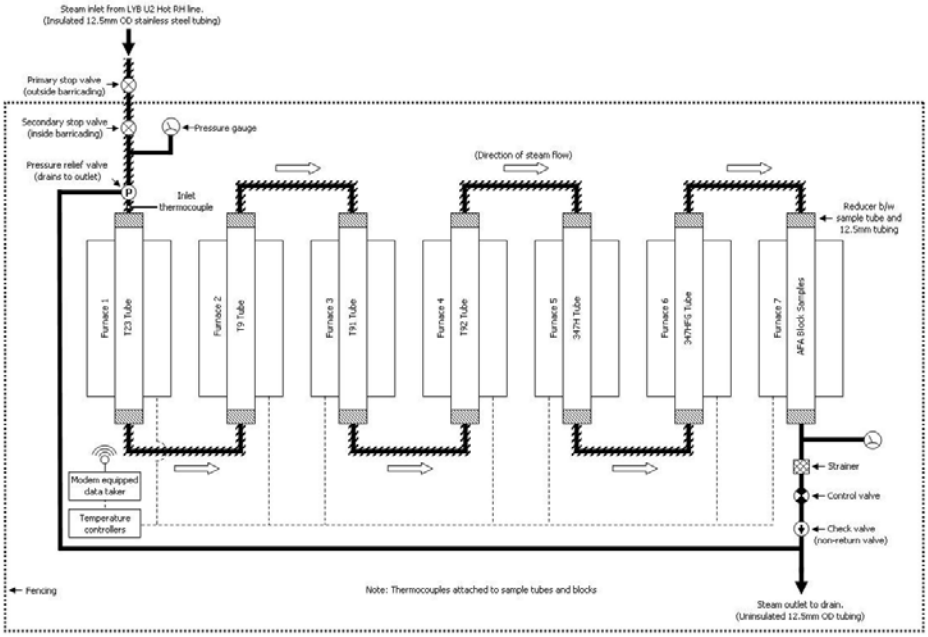

(a) Schematic showing setup of oxidation testing facility at Loy Yang B.

(b) Photograph of the live steam oxidation facility at LYB.

Figure 2 Set up of the Loy Yang B oxidation rig

Steam was tapped from the Unit 2 hot reheat line (nominally pressurised at 4.2 MPa) and channelled through seven tube samples connected in series. Each tube was installed in a three-zone tube furnace with thermocouples at 150 mm intervals along the tube such that the thermal gradient along the tubes could be accurately determined. Each tube was manufactured from a different alloy steel. The temperature range employed for each of the alloys is shown in Figure 3.

The first set of samples was removed from the setup after 4000 h exposure. The tubes were pressure welded into the system and extracting samples involved cutting each of the sample tubes in half and removing a 450 mm length for analysis. New sections of tube were then welded onto the remaining halves before testing was recommenced. The arrangement meant that following a further 8000 h exposure, one half of each sample tube accumulated 8000 h and the other 12000 h.

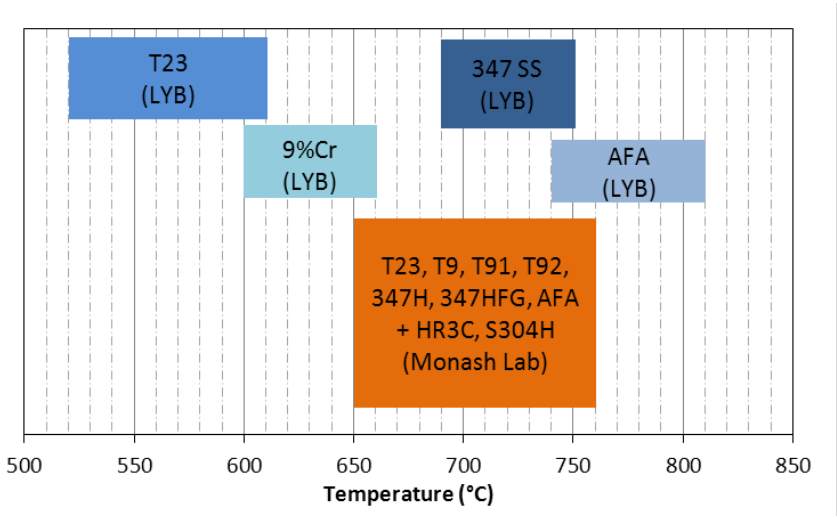

Figure 3 Temperature range employed for alloys investigated at the Loy Yang and Monash laboratories.

After exposure the oxide product was examined using optical microscopy and the thickness of the scale, which generally formed in two distinct layers, was measured directly. Laser Raman spectroscopy was used to identify the oxide phases that were present in the various scale layers. In addition the thickness of the oxide at several locations along each ferritic steel tube was measured using non-destructive ultrasonic techniques. Ultrasonic testing equipment specifically developed for the measurement of the thickness of oxides on the bore of tubing was purchased under the R&D program. The "TubeAlert" system was supplied by Aptech (USA) and this came with "TubeTech" software for temperature and life estimation. As part of the overall program this equipment was evaluated in field trials at Loy Yang A and Yallourn W power stations.

2¼ Cr ferritic steels

The typical morphology of the oxide scale formed in steam on low alloy ferritic steels consists of an inner and outer layer of magnetite (Fe_3O_4) with a thin layer of hematite (Fe_2O_3) at the steam-oxide boundary. At the metal oxide interface a chromium enriched layer of spinel ($(Fe,Cr)_3O_4$) can form in which some of the trivalent iron sites in magnetite are substituted by chromium. In addition to this, an inner layer of wustite (FeO) is expected at higher temperatures, with the wustite start temperature generally taken to fall between 580-600 °C. Wustite has the highest Fe ion diffusion coefficient of the scales mentioned and therefore offers the least protection against further oxidation. This limits the use of these materials to temperature below ~580°C.

9-12% Cr ferritic/martensitic steels

The 9% Cr steels are currently used to temperatures up to 620°C while 12% Cr materials are capable of even higher temperatures. The wustite start temperature is higher than for the 2-3%Cr alloys and these therefore show better oxidation resistance and greater creep rupture strength, making the 9-12% Cr steels the preferred class of material in many hotter regions of the steam cycle.

As in the lower chromium variants, an outer and inner layer of magnetite develops on these alloys in steam environments, however large amounts of chromium can be incorporated in place of iron in the

inner layer. The spinel layer that forms can accommodate up to 46% Cr in 12% Cr alloys compared to 13% in 2.25% Cr steels. This heavily chromium-enriched spinel oxide provides increased oxidation resistance by impeding the diffusion of iron ions to the surface, reducing the rate of growth of the outer layer.

Austenitic Steels

Austenitic stainless steels are employed where ferritic-martensitic steels are unable to withstand service temperatures. These steels are generally employed up to a practical limit of ~675°C and possess excellent oxidation resistance due to the formation of chromia (Cr_2O_3) and Fe-Cr spinel. The scale structure is similar to that of 9-12% Cr steels in that the outer layer is composed of magnetite and the inner of Fe-Cr spinel, though both form at a slower rate and with the major difference that chromia is also present. Chromia generally only develops along and around prior grain boundaries as these form pathways for chromium diffusion. This is the reason for the improved oxidation resistance reported for fine grained steels, such as 347HFG.

Austenitic steels are susceptible to exfoliation of oxide scales. This occurs because of the stress state in the scale caused by differences in the coefficients of thermal expansion of the tube metal and oxide, the volume expansion in the growing scale, the porosity of the scale and the rate of heating and cooling. A comparison of the expansion coefficients for alloys and oxides of interest over a temperature range of 0 to 600 °C is shown in Figure 4. Upon cooling, the scales that form on ferritic steels will generally possess residual tensile stresses that can lead to through scale cracking and delamination. Conversely, scales on austenitic steels contain compressive stresses, which are further exaggerated by the presence of hematite leading to an increased likelihood of buckling, shearing and spalling.

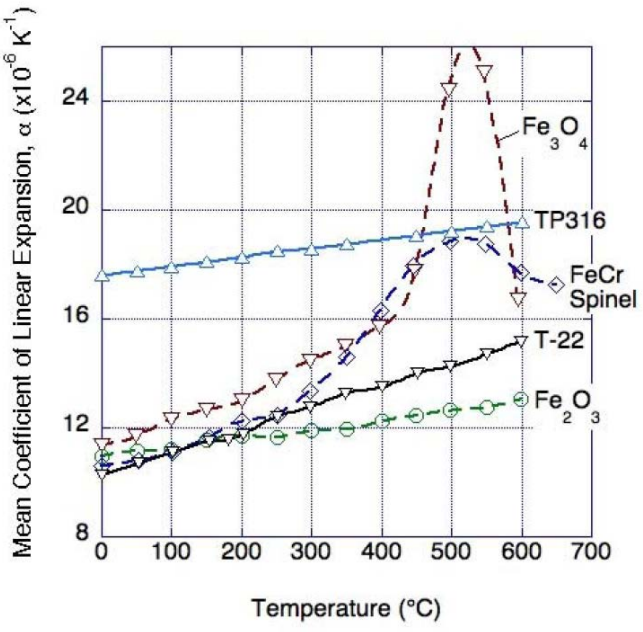

Figure 4 Coefficients of thermal expansion of Fe-based oxides and for T22 and austenitic stainless steel 316.

Oxidation kinetics

Under idealised conditions, where excess oxygen is available at the oxide surface, the rate of growth of a continuous oxide scale is determined by the lattice transport of ions through the scale. Therefore, as the thickness of the scale increases, the diffusion path increases and the rate of growth decreases. This generally leads to parabolic kinetics, where the scale thickness, x, after exposure time t, can be used to determine the parabolic rate constant, k_p according to:

$$x^2 = 2k_p t$$

In practice, scale defects such as porosity, cavities, grain boundaries, micro-channels, delaminations, cracks and exfoliation all influence ion transport. As a result, ideal parabolic rates are not always observed and the oxidation often occurs at linear kinetics at high temperatures or after prolonged exposure times. In 2.25% Cr alloys the transition to linear kinetics occurs at approximately 580-600°C. Evidence from research performed on 9-12% Cr steels indicates that parabolic kinetics govern oxidation up to 700°C and possibly 800°C.

The temperature dependence of k is most commonly described by the Arrhenius relationship

$$k = Ae^{\frac{-Q}{RT}}$$

where A is the Arrhenius constant, R is the gas constant and T is the metal temperature. Q is the activation energy for the rate controlling step of the process, typically considered to be ion transport through the scale. Thus the key parameters required for oxide thickness prediction can be determined from a plot of log$k$ against the inverse of T.

$$\log k = \frac{-Q}{R} \cdot \frac{1}{T} + \log A$$

This approach has been adopted in determining the oxidation kinetics in this work. Results for T23 and T91 alloys are included in the following plots. From these the values of constants were determined and used in the predictive algorithms. Results showed reasonable agreement between the predictions and those from other models for oxidation of these materials. Because of the extent of spallation on the austenitic steels it was not feasible to develop correlations to predict oxide thickness.

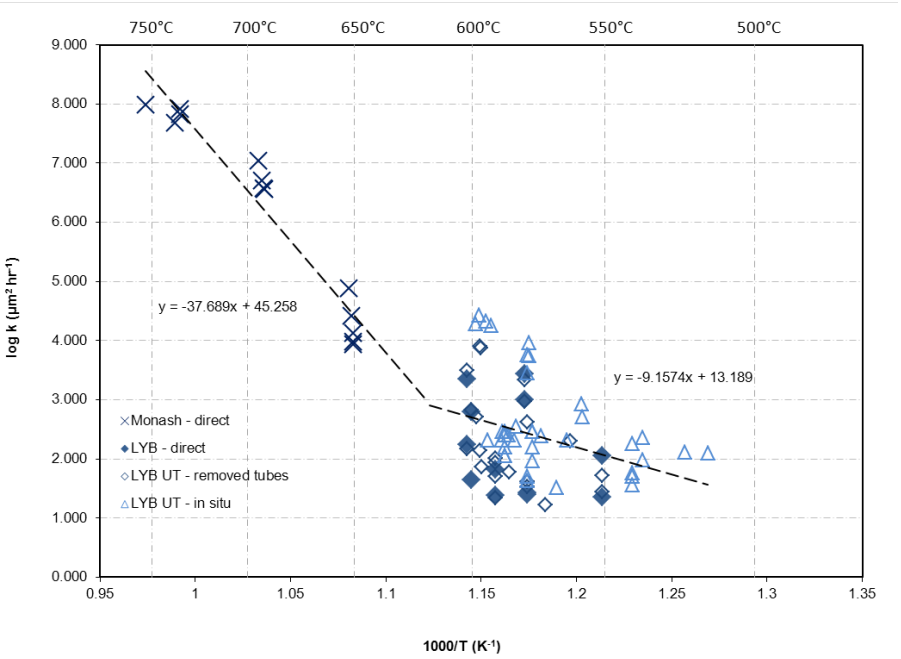

Figure 5 Plots of reaction rate constant against inverse temperature used for kinetics analysis for T23 steel, showing a change in slope, and hence in activation energy.

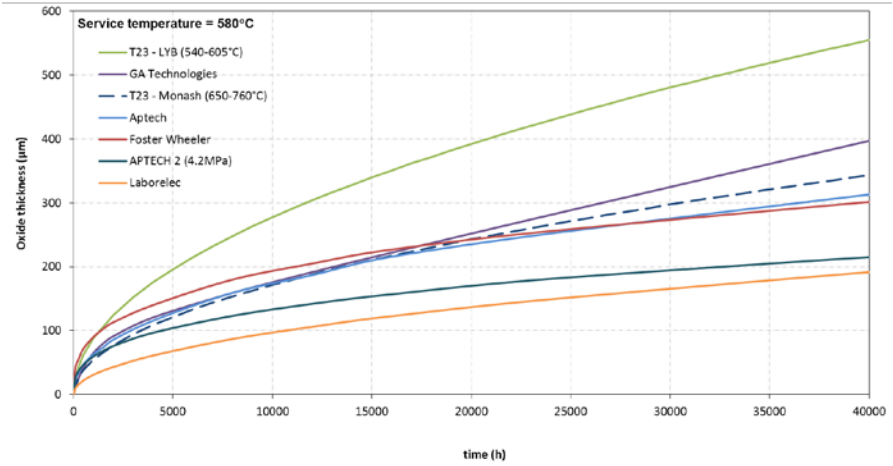

Figure 6 Oxide growth rate for T23 at 565°C as predicted from current algorithms compared with various proprietary correlations.

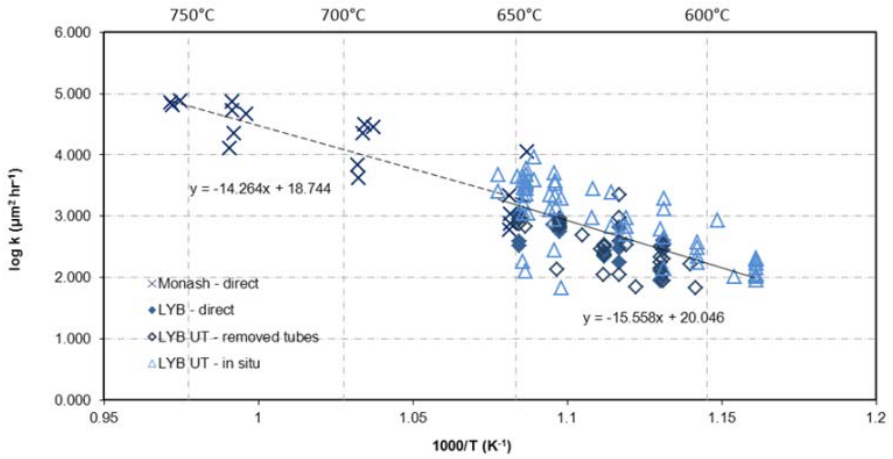

Figure 7 Kinetic data for T91 material, showing consistency between results from LYB and Monash laboratories.

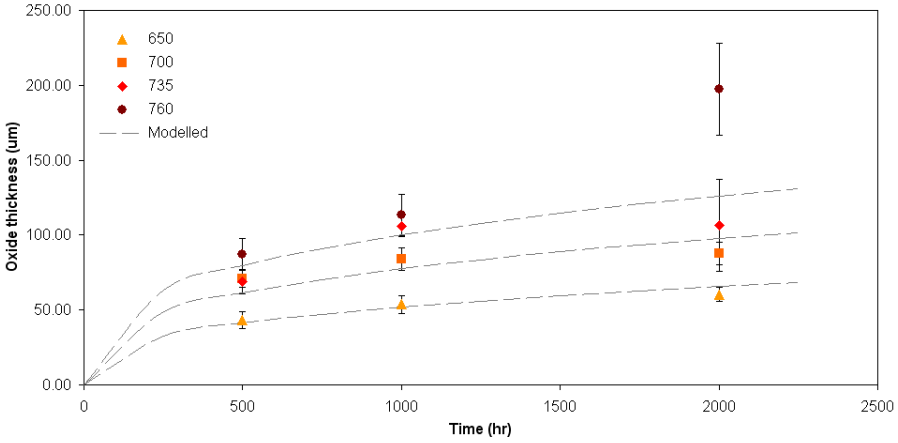

Figure 8 Inner oxide layer thickness–time data recorded for T91 showing the thickness modelled by the developed algorithms is consistent with actual data.

A significant improvement in oxidation resistance was recorded for T91 over T9. This is surprising given that the additional Nb and V alloying content in T91 is primarily designed for precipitation strengthening and improved creep resistance through carbide and nitride stabilisation at elevated temperature. The improved resistance to oxidation may nevertheless be attributed to microstructural refinement by niobium carbides which are extremely stable and do not dissolve at normal austenising temperatures. Undissolved niobium carbides are thus able to restrict grain growth and produce a refined prior-austenite grain size compared to T9, facilitating easier transport of Cr to the metal surface in a similar way to that described for fine grained austenitic material.

The key outcomes from this first Strand of the program included:

- Development of kinetics algorithms for advanced alloys which compare well with models for similar alloys available in literature.
- Of the 9% Cr alloys it was found that T9 showed least oxidation resistance. T91 exhibited highest oxidation resistance but was most prone to scale exfoliation. T92 developed scale that was less regular than other 9Cr variants.

- The activation energies (mechanisms) observed for T23 below and above wustite start temperature were quite different, as expected. The presence of tungsten does not appear to have a significant influence on oxidation kinetics; i.e. the results for T22 were similar to those for T23 reported in the literature.
- Stainless steels develop irregular scales that are not suitable for analysis by thickness measurements. AFA and HR3C showed the best oxidation resistance, particularly at temperatures associated with USC applications.
- Field and laboratory testing of the bore oxide thickness UT equipment provided confidence that results were reliable and reproducible.

8 Strand 2 - Microstructural changes

The microstructural transitions in a range of alloys that are used, or could be used, in fossil plant were investigated after extended high temperature exposure for times up to 20,000 hours. An improved understanding of these changes, and particularly the ability to quantify the changes to some extent, enables the condition, life and fitness for service of thermally degraded alloy steels in power plant to be determined, and for appropriate inspection, refurbishment and replacement to be programmed.

The results from the program are presented in the form of an atlas of microstructures for each of the alloy groups that were evaluated, i.e. 2¼Cr and 9Cr ferritic steels and the austenitic steels. Some general comments on the microstructure and associated hardness transitions are included below.

2¼%Cr steels

Grade 23 is a ferritic steel with improved elevated temperature creep rupture strength over the older 2.25Cr-1Mo (T22) steel and differs in chemical composition through the substitution of tungsten for molybdenum. Tungsten is superior to molybdenum in impeding the formation of M_6C during long term high temperature exposure. The microstructure of T23 consists of a bainitic matrix strengthened by $M_{23}C_6$ carbides located mainly along grain boundaries and finely dispersed vanadium carbides in the matrix which are fine and stable even after long term high temperature exposure. Another feature of T23 material is its tolerance to heat treatment and the lack of post weld heat treatment required for thin-walled structures.

Ageing of the T23 steels resulted in the $M_{23}C_6$ grain boundary carbides coarsening and the granular bainite degrading with the prolongation of aging time. The coarsening of the $M_{23}C_6$ carbides occurs early in the ageing process with the degradation of bainite occurring after longer-term ageing such that bainite-residuals completely disappear after 8,000 hours at 600°C. The material is only suited to service at up to approximately 650°C and it, not surprisingly, showed rapid deterioration at 700°C. The material exhibited softening consistent with the microstructural changes, as can be seen in Figure 9 where hardness is plotted against the Larson Miller parameter[2].

[2] The Larson Miller Parameter (LMP) combines the effects of temperature and time of exposure. Although normally used for creep life projection it is equally valid for other thermally activated processes such as tempering. Generally the LMP has been determined using C = 20 although in some instances improved regression coefficients were achieved with alternative values for this constant.

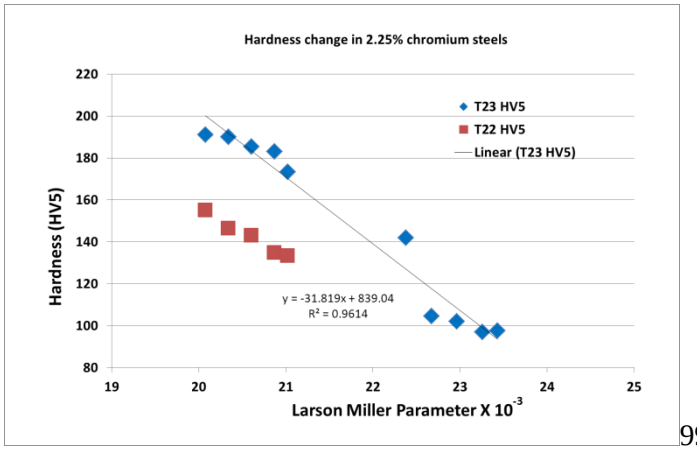

99

Figure 9 Hardness versus LMP for T22 and T23 steels

9%Cr ferritic/martensitic steels

The microstructure of the 9%Cr steels consists of a tempered martensite with fine carbides (MX and $M_{23}C_6$) on the martensite laths. Nucleation of Laves phase and Z phase can also be observed after exposure at 600°C and above.

In the 1980s T91 was developed with improved creep strength compared to T9. The increased strength results from precipitation strengthening by fine MX carbo-nitrides, a consequence of the addition of vanadium and niobium. It is well known that the fine MX carbo-nitrides of niobium and vanadium are very stable at elevated temperatures and contribute significantly to increasing creep strength. A complication in the use of the 91 grade steels is its need for accurate temperature control during welding and post weld heat treatment for even thin sections. Traditionally, the 9Cr steels have been very hard to assess as the microstructure, as determined using optical microscopy, does not change significantly.

A recent development has been an improved 9Cr steel called T92, which has better weldability but still requires tight control for pre and post weld heat treatment.

With ageing at 600°C for up to 16,000 hours there was no significant change to the microstructure of T9. There was significant coarsening of $M_{23}C_6$ and Laves phase at the lath boundaries following the apparent diminishing of the boundaries. The lath boundaries were completely dissolved at 16,000 hours leaving only prior austenite grains. For exposure at 700° the T9 microstructure changes little after 4,000 hours exposure, apart from a slow coarsening of the carbides.

Similar observations pertain to the T91 and T92 materials. For T92 there was slight grain growth with time when aged at 700°C and visible precipitation of most probably $M_{23}C_6$ and Laves phase at the lath boundaries. The martensite lath boundaries were clearly evident after 1,000 and 2,000 hours but become less clear after 4,000 hours exposure and disappear after 12,000 hours exposure. After 12,000 hours the precipitates within the grains were quite evenly dispersed. Hardness changes were seen to offer more information on the material degradation than could be discerned from optical microscopy. Data showing similar trend lines for the various 9%Cr alloys is presented in Figure 10.

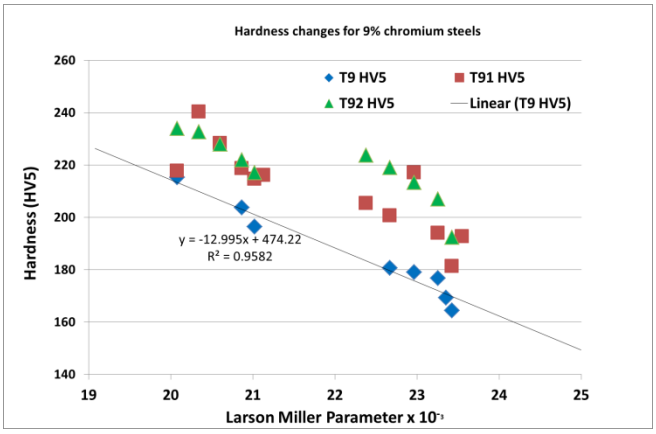

Figure 10 Hardness versus LMP for P9, P91 and P92 steel. [Default LMP constant C = 20].

Austenitic stainless steels

347H (18Cr-12Ni-Nb) and 347HFG

347H is an austenitic stainless steel with 0.8wt% Nb that was developed to improve the resistance to sensitisation and thus avoid severe intergranular corrosion and cracking. It is widely used for superheater and reheater tubes in boilers. Improvement of 347H has led to the development of 347HFG by grain refinement through a thermo-mechanical process leading to better oxidation resistance. The microstructure consist of a fine-grained austenitic matrix strengthened by $M_{23}C_6$ carbides on the grain boundaries and finely dispersed NbC carbides in the matrix.

HR3C (25Cr-20Ni-Nb-N)

HR3C steel has been widely used in superheater and reheater tubes in ultra-super critical power plants due to its superior corrosion resistance at high temperature. The creep strength is achieved by its finely dispersed $M_{23}C_6$ and NbCrN precipitates. However, the creep rupture strength is not as high as other alloys and thus requires an increase of tube wall thickness and higher production cost.

SUPER304H (18Cr-9Ni-3Cu-Nb-N)

Super 304H is an austenitic stainless steel with 18% chromium and 9% nickel (compared to 8% Ni for SA-213 TP304H). The increased oxidation limit and corrosion resistance of Super 304H compared to 304H is attained through the addition of copper, niobium and nitrogen as well as the higher nickel level. Super 304H is stronger at elevated temperatures than either 304H or 347H due to the strengthening effect of fine Cu-rich precipitates, which are formed in the temperature range of 580°C to 640°C. As a result, Super 304H is applicable for ultra-supercritical boilers.

AFA (20Ni-12-14Cr-2.5-4Al)

Alumina forming austenitic (AFA) stainless steel is an alloy recently developed by Oak Ridge National Laboratory that has promising oxidation resistance up to 800°C. The high aluminium content promotes the formation of an alumina scale, rather than the chromium oxide or iron-chromium spinel that typically forms on stainless steels. The alumina scale is more stable and protective than chromia scales. AFA is also said to have good creep strength resulting from the formation of NbC carbides and intermetallic phases such as AlN, displaying excellent creep strength at temperatures up to 800°C. The ductility is reportedly low.

In the authentic steels there was little consistent change in hardness with exposure time, and there was no significant difference in hardness between the various alloys that might reflect the range of creep strengths. The hardness data is shown for all the austenitics in Figure 11. A concern with long term exposure of some austenitic stainless steels at elevated temperature is the tendency for the embrittling sigma phase to develop at grain boundaries (Figure 12). This was observed in the 347H and 347HFG steels, with both showing similar volume fractions at 10,000 hours exposure.

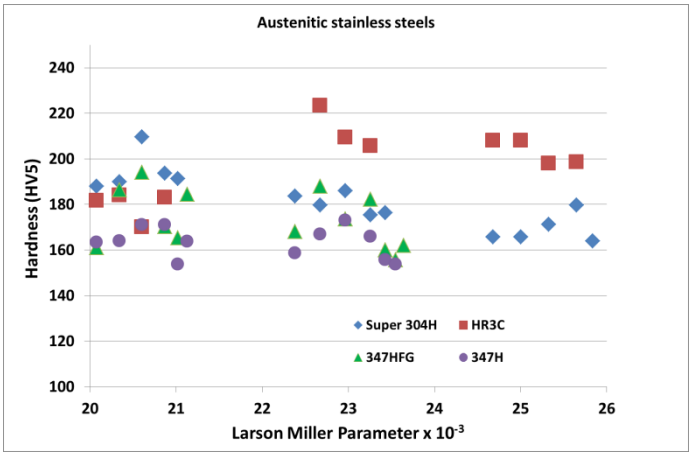

Figure 11 Hardness data for austenitic alloys after exposure at temperatures from 600°C to 800°C, showing little consistent trends. [LMP constant C = 20]

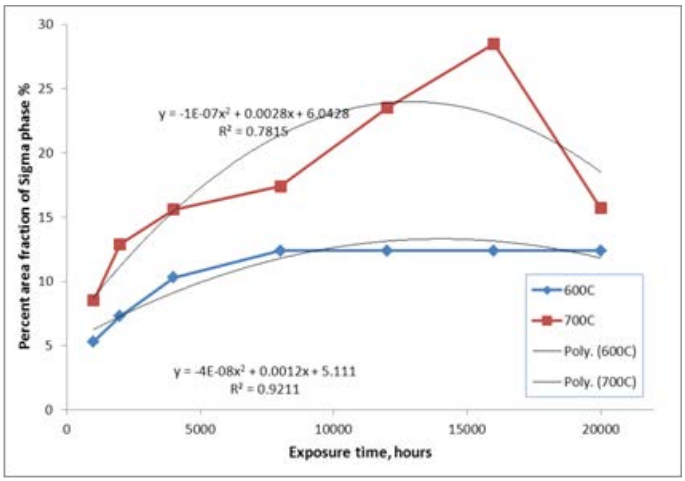

Figure 12 Sigma phase development in 347HFG at 600°C and 700°C

9 Strand 3 - Creep strain assessment

A testing facility and suitable test procedures have been developed to undertake creep testing and the measurement of creep strain rate. Other researchers have developed alternative techniques for creep life assessment based on strain rate data and these were evaluated against results from more conventional time-to-rupture testing. Sufficient strain rate data for the assessment of the remaining creep life can be obtained with relatively short term tests – i.e. less than 1000 hours. These techniques were evaluated to determine whether or not the more rapid creep-strain techniques are valid and provide an accurate assessment of remaining life.

When a steel is loaded to sufficiently high stress at elevated temperature it will experience permanent and continuing time-dependent deformation called creep. There are three identified stages of creep, determined by the strain rate, as shown in the graph opposite. When load is first applies during the primary stage the strain rate decreases to approach the minimum, steady state rate of secondary creep. In the testing of many alloy steels the secondary stage occupies the bulk of the creep life period. As the extent of creep damage accumulates the creep strain rate accelerates into the tertiary stage, leading to final rupture.

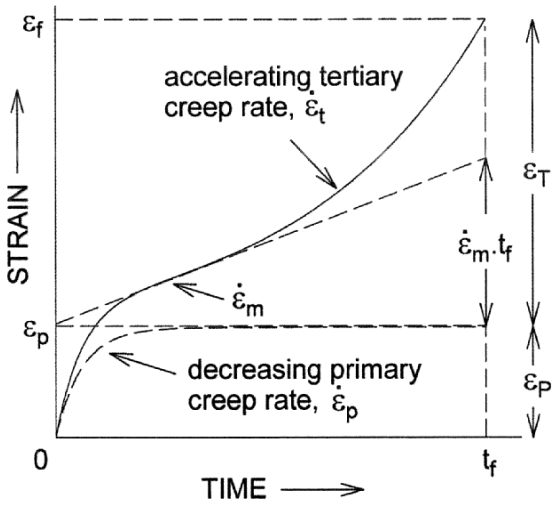

Many have held the mistaken view that tertiary creep was caused by necking, micro-cracking, or other geometrical changes. In fact, it has been shown that when a material is in the tertiary phase of its life, the rate of creep acceleration with strain is constant, and can be expressed mathematically as a material property, and is the basis of some creep assessment models. This strand of the R&D program was developed to investigate two emerging methods for experimental life assessment, the Theta Projection method and the Omega method. The Omega method has recently been incorporated into API 579 – Fitness for Service and thus has reasonable credibility.

The creep testing was carried out using an Instron 1362 creep fatigue machine, which has the capability of maintaining constant load on a standard test piece whilst monitoring the creep strain. The test specimens were cut from heavy sections of CMV and P22 pipe that had been in service for 213,000 hours and 143,000 respectively. Creep rupture testing was carried out to provide data on the current creep strength and remaining life of these materials consumed as a result of service exposure. Creep strain testing and the complex calculations required for the theta and omega methods were concluded and the remaining life estimates were compared with the traditional test results.

Examples of the results from creep testing on P22 and CMV materials are included in Figure 13. It is important that the testing conditions are such that creep enters the tertiary phase, and that there is an acceleration of creep strain rate during the test. This was quite pronounced in tests on the CMV and can be seen to a much lesser extent in some of the T22 results for tests at the higher temperatures.

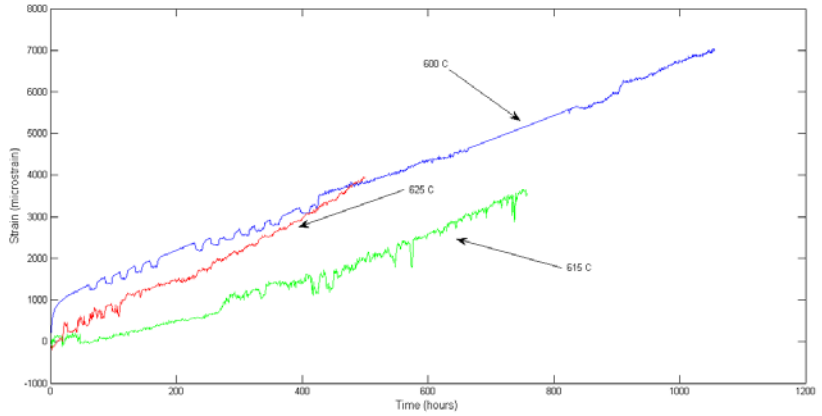

(a) P22

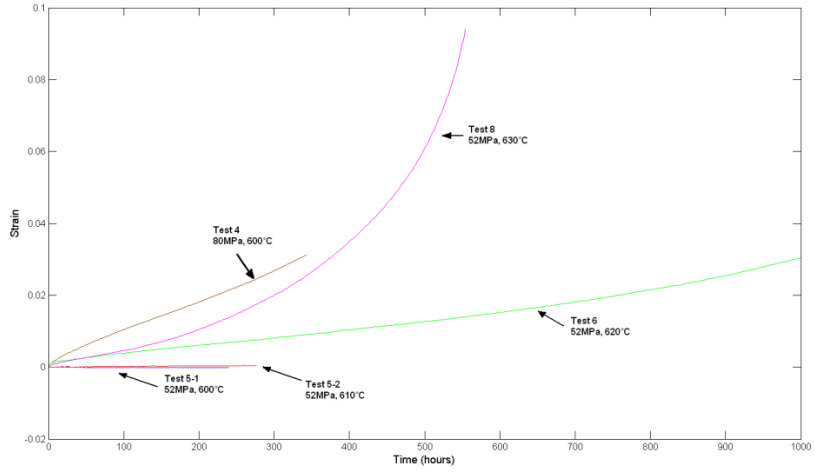

(b) CMV

Figure 13 Creep strain data for tests on P22 and CMV samples showing clearly accelerating strain rates in long term tests on CMV, and to a lesser extent for the higher temperature tests on P22

It can be seen from the five successful CMV test that strains of approximately 3% to 10% were achieved by the end of the tests, except for Test 5-1 and Test 5-2 where no significant strain at all was measured. Tests 4, 6 and 8 passed through the secondary creep region (where the minimum creep rate occurs) and entered the tertiary region. This allowed the Theta and Omega methods to be used.

The accelerated creep rupture testing that was carried out on the P22 attemperator pipe confirmed it had sound creep properties, consistent with the mean properties for P22. This is consistent with the relatively low operating temperature in-service. From extrapolation of the test data the estimated life fractioned consumed ranged from 44% to 65% and the predicted service life at the normal operating temperature of 490°C was 2.3 – 5.2x10^6 hours. Creep rupture testing on the CMV material showed considerably greater creep deterioration compared to the virgin material mean properties. The estimated life fraction that had been consumed in service was 83%. The projected remaining life of the CMV at

service temperature of ~540°C was 260,000 hours[3], assuming that hoop stresses in the Y-piece were 52 MPa, rather than 75 MPa as was used in the creep rupture testing, making allowance for stress concentrations from the complex geometry.

Creep test conditions for the Omega and Theta comparisons are included in Table 2 together with life fraction consumed based on Theta and Omega calculations. It was possible to develop a suitable equation to extrapolate the Omega results back to the operating temperature, and the results for remaining life are included in the Table. Due to the limited data and the large extrapolation range this was not the case for the Theta Projection results.

Results from the first three tests on the P22 material generally showed an underestimation in the remaining life using both the Theta and Omega methods. This seems likely to be a result of the low levels of accumulated strain in the tests – i.e. the tests did not run for a long enough time or could have been conducted at higher temperature or stress to achieve the necessary strains of around 10% that are necessary for reliable calculations using these methods.

Results from the CMV tests showed reasonable agreement with predictions of life fraction consumed from creep rupture tests for both the Theta and Omega methods. It should be noted that the CMV tests generally reached much higher levels of strain than the P22 tests and thus a larger portion of the tertiary region of creep was sampled enabling more accurate life prediction. The estimation of remaining creep life at operating temperatures is a more important output from the calculations, and the results for CMV are reasonably consistent with the estimated life of 260,000 hours. The extensive remaining life of the P22 material is predicted by the Omega method, although these should be considered to be relatively theoretical – testing would never approach such times!

Test number	Material	Temperature	Stress	Test duration	Mean life	Omega method			Theta method	
						Remaining life - test	Life fraction consumed	Remaining life - op'n	Remaining life - test	Life fraction consumed
		Deg C	Mpa	hours	hours	hours		hours	hours	
1	P22	600	60	1000	13,892 9,247 11,730	-		-	18,796	0%
2	P22	615	60	750	6,032 4,009 5,134	1,129	78%	6,770,000	2,338	54%
3	P22	625	60	500	3,459 2,297 2,960	990	66%	11,640,000	2,330	20%
4	CMV	600	80	344	7,276	493	93%		1,756	76%
5-1	CMV	600	52	239	41,368	-	-	-	-	-
5-2	CMV	610	52	275	23,856	-	-	-	-	-
6	CMV	620	52	1000	13,957	1,537	89%	294,000	3,210	77%
7	CMV	630	52	70						
8	CMV	630	52	555	8,281	683	92%	230,000	869	90%

Table 2 Details of each of the creep test conditions, together with various estimates of the mean creep life at test conditions based on various master creep curves. The life fractioned consumed as determined using the omega and theta methods is included and the projected remaining life at the normal operating temperature was determined using the Omega method.

[3] This was determined from calculations using mean creep-rupture data based on a master curve developed by EEEC.

The Omega method appears to be more powerful for remaining life assessment because it can give a remaining life at operating conditions from just a single creep test. Using the Theta Projection method requires multiple tests so that an accurate value for theta can be determined, and may also require knowledge of the materials rupture strain at test conditions. The other significant advantage for the Omega method is that it requires no prior knowledge of the operating history of the exposed material; accurate temperature data and operating time are not required for an Omega assessment, although the life will be estimated for the normal operating temperature. Nor does it matter if the operating temperature varied throughout the material life as this method simply considers the remaining 'damage resistance' of the material. All these factors make Omega potentially a more powerful method for the purpose of remaining life assessment of post exposed plant material.

Some more targeted testing would be warranted to better establish the optimum and minimum creep testing strains that are necessary to ensure the life prediction is accurate and consistent. This would allow a more meaningful comparison of the relative merits of the Omega and Theta projection methods. With the extensive background information that has been developed in the ETIS/BCIA program, and the relatively short test periods required, a focussed program could be finalised with a 12 month program.

10 Strand 4 - Welding repair technology

The key objective of this aspect of the research program was to determine if weld repairs using the flux-core arc welding (FCAW) procedure could be used in place of conventional manual metal arc welding (MMAW). The two processes are compared in the schematic below.

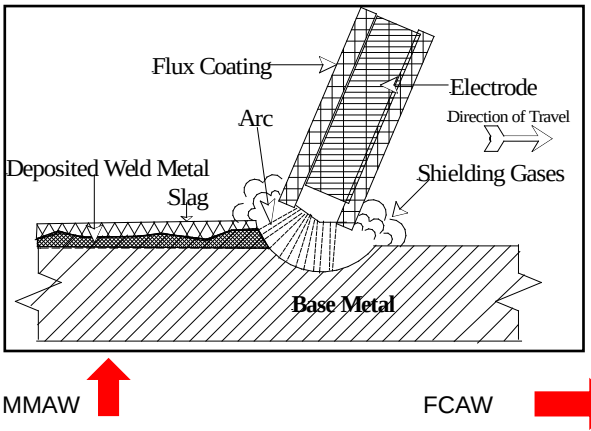

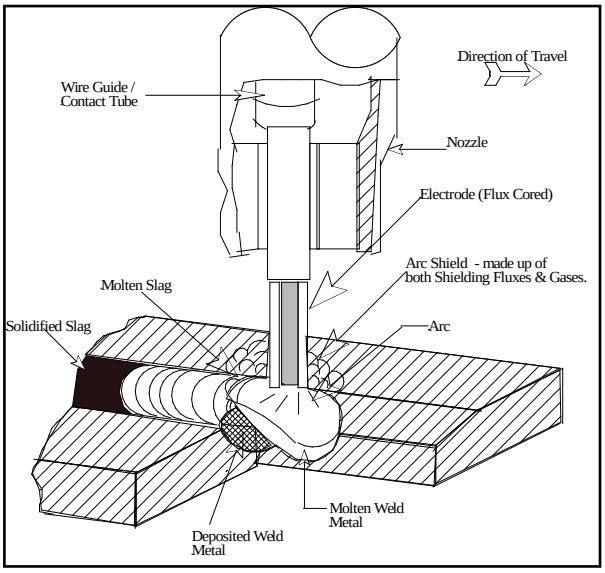

FCAW is a semiautomatic process that uses flux-cored electrodes that are meters long, contrasting with MMAW that is manual and uses electrodes that are just centimeters long and coated with flux on the OD.

The flux-cored technology allows more rapid weld metal deposition, and hence can lead to reduced time for weld repairs. Testing was conducted to quantify the creep performance of welds in 2¼Cr1Mo steel (P22) and in chromium-molybdenum-vanadium cast steel (CMV), both of which had seen extensive service life. Tests were also carried out on welds in one of the 'second generation' high temperature steels, a 9Cr1Mo steel (P91), which has improved high temperature strength compared to the P22 and CMV material. Where appropriate the welds in the three alloys were considered after a conventional post weld heat treatment and also after welding using the temper bead approach, where successive weld runs effectively temper and condition the earlier runs and this improves the properties of the weld.

Temper bead welding (TBW) is particularly suited to in situ weld repairs where access or structural integrity preclude a full post weld heat treatment, which requires heating to around 700°C.

Samples for creep rupture testing were taken from across the welds, so as to include parent metal, heat affected zone and the weld metal itself (Figure 14). Of interest from the rupture testing was not only the

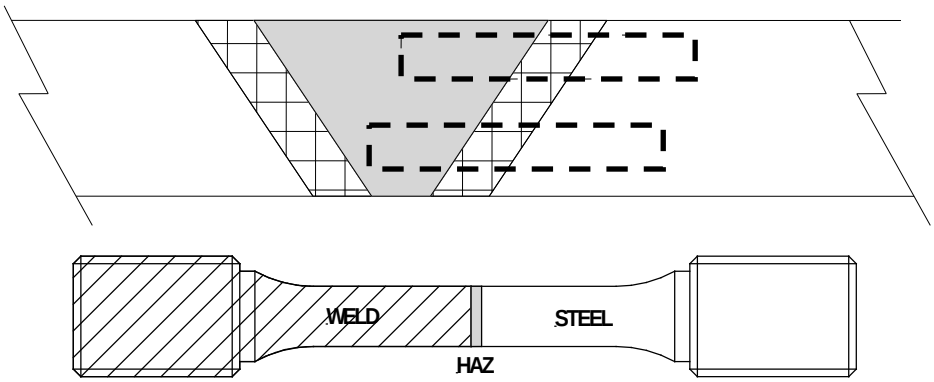

Figure 14: Test-piece orientation with respect to the weld fusion line and HAZ showing a longitudinal sample with half sample parent metal and HAZ

time to failure (at the given temperature and stress) but also the location of failure – to establish if there was any indication of inherent weakness or embrittlement and cracking susceptibility in the heat affected zone.

2¼Cr1Mo

The low alloy chromium molybdenum steel (P22) was taken from service exposed attemperator piping (600 diameter x 48 wall thickness) after approximately 143,000 hours at around 490°C. The weld preparation involved machining a groove 46 mm deep, as shown in Figure 15. Each quadrant of the sample was welded using a different procedure - FCAW and MMAW using standard or temper bead techniques. After welding the pipe was cut and appropriate samples were given a standard post weld heat treatment.

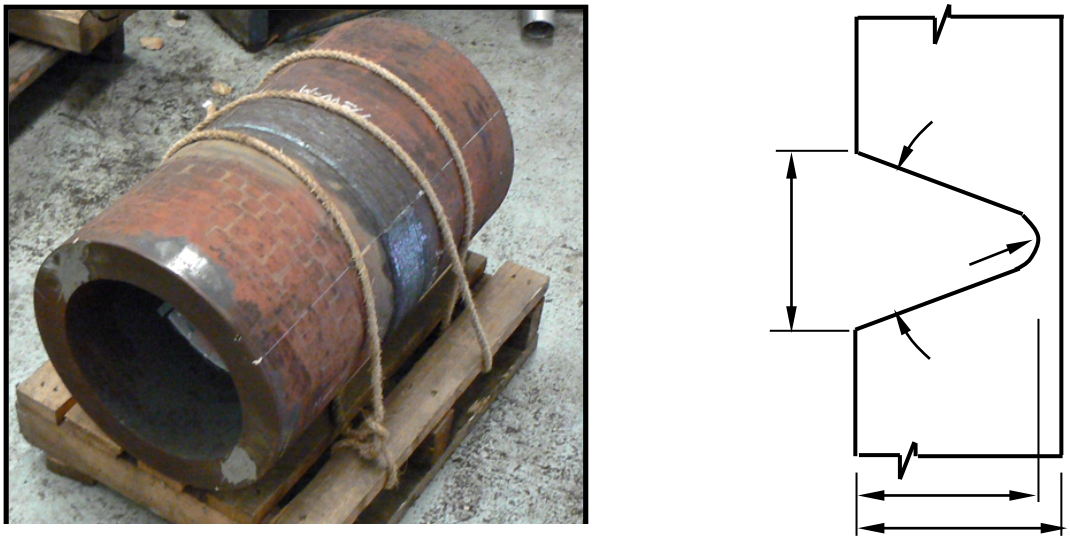

Figure 15 Sample of P22 pipe after welding and sketch showing the weld preparation.

At the relatively low operating temperature for this material little deterioration of creep strength was expected. The testing of miniature creep rupture samples confirmed that the creep strength was consistent with the mean creep properties of unexposed material. Results from tests on cross weld samples at a stress of 62 MPa and at 80 MPa are compared with the mean data in Figure 16. The creep strength of the welded samples is significantly lower than that of parent material, and this is expected as the cross-weld test pieces tended to fail within the weld metal itself. Weld creep strength was above the lower bound predicted strength for virgin material. Although there were limited tests completed there does not appear to be any significant difference in the creep strength between weld procedures or with PWHT or TBW.

Residual stress and hardness tests on the welds were carried out. Residual stresses at the weld surface were relatively low, but more meaningful measurements were taken after removal of 4 mm of metal. Very high residual stress (~ 400 MPa) existed after temper bead welding for both MMAW and FCAW. Post weld heat treatment reduced the residual stress levels to less than 50 MPa. Hardness testing reflected the stress data and hardness of weld metal after TBW peaked at 320HV while hardness through the HAZ was less than HV270. There was no apparent difference between FCAW and MMAW.

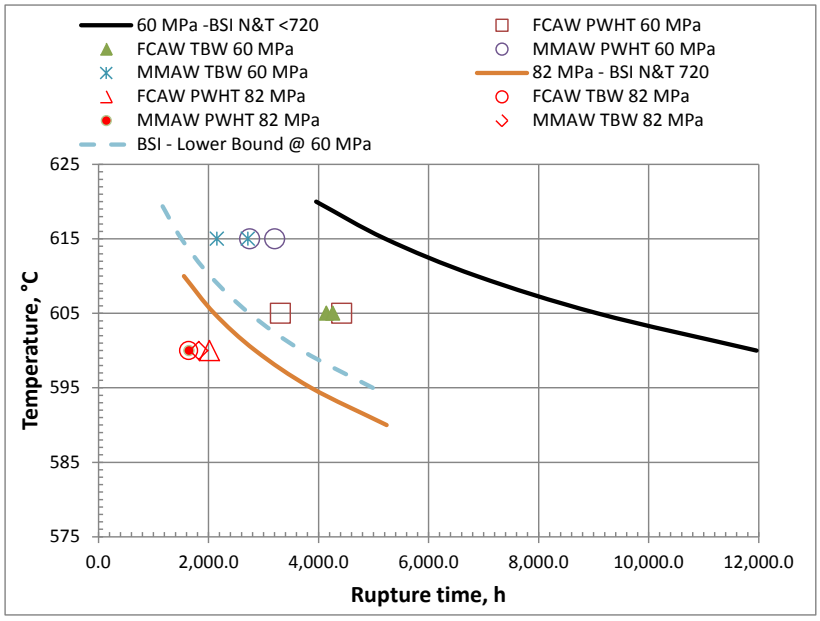

Figure 16 Creep rupture results for tests on welded P22 materials. The creep strength of welds is lower than that of parent material.

½Cr ½Mo ¼V

The CMV material was removed from a bifurcation in a main steam line. The cast 'Y-piece' was taken out of service as a result of cracking at welds after more than 200,000 hours service at mean steam temperature of 540°C. A significant reduction of creep strength would be expected after this service.

The material was generally in excess of 100 mm in thickness and a similar weld preparation groove was machined across a section of the Y piece. The very thick sample (Figure 17) provided extensive material for cross weld testing.

A very consistent data set for the CMV confirmed that the creep properties of the as-received material were less than the lower bound properties for CMV. This was not unexpected and is probably a result of the extended service to date and the fact that the component was a casting, and the creep performance of cast materials is generally inferior to wrought components, such as piping. The cross-weld test results showed that the welding did not reduce the creep performance. The creep rupture strength of either MMAW or FCAW combined with PWHT or TBW was consistent with the creep rupture results for the parent material.

Figure 17 One of two CMV samples after completion of welding activity

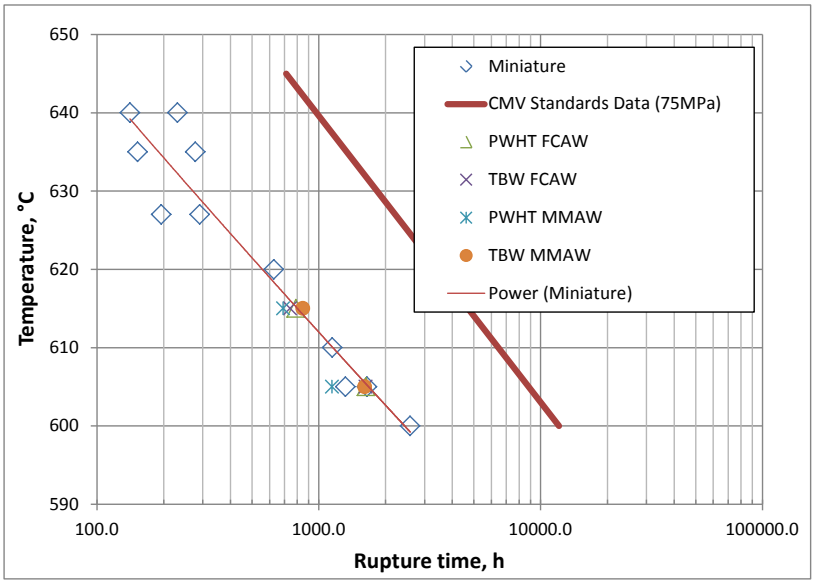

Figure 18 Results from creep rupture testing on parent CMV metal (identified as miniature) and cross weld samples compared with mean creep strength curve for wrought CMV.

The residual stress levels in the CMV welds were higher than those in P22, and high stress were also present at the surface, ie without removal of metal. The highest stresses were parallel to the welds and the maximum recorded was 536 MPa, for TBW samples. There was not enough data to confidently assess whether or not there were differences in stresses or hardness in the FCAW compared to MMAW, but this did not appear to be the case.

9Cr1Mo

The outcome of the creep rupture testing on P91 FCAW and MMAW welds was similar, although there is some scatter in the test results. Additional work would be required to determine whether or not the creep strength using FCAW or MMAW is significantly different. The data confirmed that the parent material exhibited creep strength in excess of the mean property, but the cross weld samples showed considerably lower creep strength, although this was always above lower bound figures.

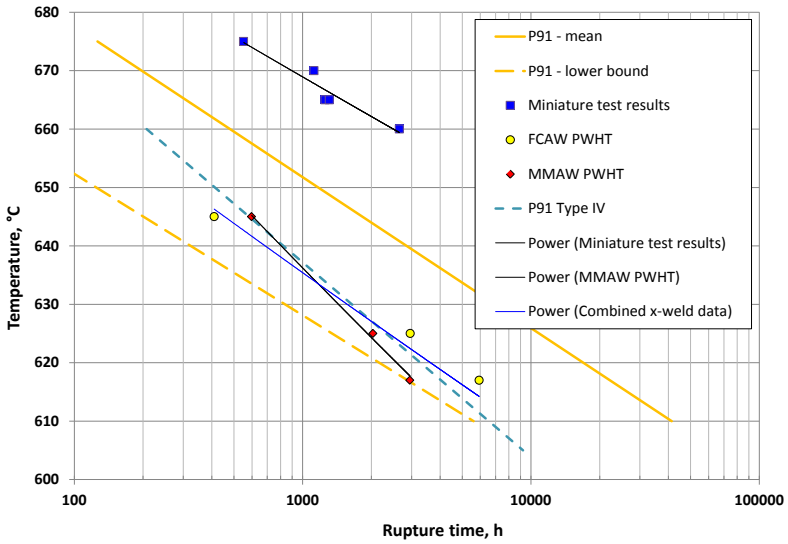

Figure 19: Results for the Grade 91 creep tests showing parent metal to have creep strength above mean properties and welds to be above lower bound..

The creep rupture testing carried out on the cross weld samples was of relatively short duration, up to 4500 hours, which was necessary to complete the extensive test program in the allotted time. As noted, the results to date indicate that flux cored welding, with either full PWHT or carried out using the temper bead approach, appears to offer similar high temperature creep properties to conventional weld repairs. Longer term testing would significantly improve confidence in this finding. A longer-term creep rupture program targeting rupture times up to ~20,000 hours could be undertaken to improve the data set and allow more accurate extrapolations to determine the typical life of these welds at normal service conditions. Considering the potential savings from reduced outage duration for weld repairs that FCAW might offer, such additional testing would appear to be justified.

11 Inputs from participants

The major power generation companies in Victoria's Latrobe Valley made significant investments in the Advanced Materials Assessment R&D Program, both in the form of financial contributions and access to facilities and personnel. Their key contributions are gratefully acknowledged.

International Power – Loy Yang B

Provided access for the steam oxidation facility, welding services for installation of test samples, labour to remove and re-install test sections, power plant data on steam temperature and pressure, valves for safe isolation of the test facility. Personnel to oversee the safe operation of the facility.

International Power - Hazelwood

Welding and post weld heat treatment of aged 2¼Cr1Mo material using both flux cored and conventional MMA welding techniques and temper bead and full PWHT.

Loy Yang Power

Supply of aged 2¼Cr1Mo material from replaced attemperator for welding assessments. Provision of U-bend tubing and samples for the steam oxidation testing. Welding of P91 ferritic alloy steel piping

with flux cored and MMA welding procedures and full PWHT. Opportunity to benchmark oxide thickness against tubing with known temperature history from in-plant bore oxide surveys.

TRUenergy Yallourn

Supply of aged CMV bifurcation from the main-steam line for weld tests. Machining and welding of samples using both flux cored and conventional procedures. Bore oxide surveys of convention pass tubing.

Monash University

Oxidation test facility for laboratory exposure. Masters program and supervision for oxidation work, including Raman spectroscopy to characterise oxides.